Absolute TiN(111) Step Energies from Analysis of Anisotropic Island Shape Fluctuations

S. Kodambaka, V. Petrova, S. V. Khare, D. D. Johnson, I. Petrov, and J. E. Greene

Department of Materials Science and the Frederick Seitz Materials Research Laboratory,
University of Illinois, 104 South Goodwin Avenue, Urbana, Illinois 61801
(Received 19 December 2001; published 20 March 2002)

In situ high-temperature (1165–1248 K) scanning tunneling microscopy was used to measure fluctuations around the equilibrium shape of two-dimensional vacancy islands on TiN(111) terraces. From the equilibrium shape, the ratio of the two $\langle 110 \rangle$ step energies was found to be 0.72 ± 0.02. Combining this with the results of an exact approach for analysis of shape fluctuations, applicable to highly anisotropic islands, we obtain absolute values for step energies and step stiffnesses as a function of orientation.

NaCl-structure titanium nitride (TiN) is widely used as a hard, wear-resistant coating on cutting tools, as a diffusion barrier in microelectronic devices, and as a corrosion and abrasion resistant layer on optical components. Even though its elastic and diffusion-barrier properties are highly anisotropic, and hence depend strongly upon film texture, the mechanisms and reaction paths leading to the development of preferred orientation in polycrystalline TiN layers are not understood. Efforts to model these processes [1] require, as input, detailed knowledge of adatom transport parameters and surface site energies. Here, we focus on the step formation energy.

The step formation energy β as a function of step orientation φ is a fundamental parameter used to describe crystal surfaces. $\beta(\varphi)$ is the two-dimensional (2D) analog of the surface free energy $\gamma(\varphi)$. Just as $\gamma(\varphi)$ determines the equilibrium shape of bulk crystals, the variation of β with φ determines the equilibrium shape of 2D islands on a terrace. A related property, the step-edge stiffness, $\tilde{\beta}(\varphi) \equiv \beta(\varphi) + d^2\beta(\varphi)/d\varphi^2$, is proportional to the island chemical potential [2] and hence controls island coarsening and decay kinetics. Unfortunately, very little data, either experimental or theoretical, are available concerning $\beta(\varphi)$, even for elemental metal surfaces. For more complex materials such as transition-metal nitrides, there are no published data.

Experimental determination of orientation-dependent step energies is difficult. An "inverse" Wulff plot [2,3] constructed from direct measurements of the equilibrium shape of 2D islands yields only the *relative* orientation dependence of step energies. Additional experiments are necessary to determine *absolute* values of $\beta(\varphi)$. Bartelt *et al.* [4] used step fluctuation measurements for Si(001), while Bonzel and co-workers [5] employed 3D equilibrium crystal shape measurements and surface energies for Pb(111). Icking-Konert *et al.* [6] described a method to determine absolute $\beta(\varphi)$ values from the temperature dependence of equilibrium island shapes. Recently, Schlößer *et al.* [7] have shown that shape fluctuation measurements of isotropic (circular), or near-isotropic, islands at a *fixed* temperature can be used to determine absolute average step energies, thus eliminating the need for additional

experiments. This technique, however, is not applicable to obtain $\beta(\varphi)$ for anisotropic island shapes.

In this Letter, we present a new approach for the analysis of shape fluctuations, applicable to both isotropic and highly anisotropic islands, and apply it to the determination of absolute $\beta(\varphi)$ values from high-temperature scanning tunneling microscopy (STM) measurements of the equilibrium 2D vacancy island shape, and temporal fluctuations about that shape, on atomically smooth TiN(111) terraces. We derive an analytical expression for the orientation dependence of $\beta(\varphi)$ from the equilibrium shape using the inverse Legendre transformation [2,3]. This provides relative $\beta(\varphi)$ values within an orientation-independent scale factor λ, the equilibrium island chemical potential per unit TiN molecular area, while eliminating the conventional inverse Wulff construction which involves the tedious procedure of tangent constructions. Next, we derive an exact expression relating the temporal change in island free energy, a function of λ, to thermal fluctuations around the equilibrium shape. From the STM shape fluctuation measurements we determine, using our analytical formulation, λ and hence absolute values for $\beta(\varphi)$. Our approach makes no assumptions, as required in earlier analysis [8], regarding island isotropy.

Epitaxial TiN(111) layers, 2000 Å thick, were grown on Al$_2$O$_3$(11$\bar{2}$0) by ultrahigh vacuum (UHV) magnetically unbalanced magnetron sputter deposition [9] using the procedure described in Ref. [10]. The samples were transferred to a UHV multichamber variable-temperature Omicron STM with a base pressure of 2×10^{-10} Torr. The system is equipped with facilities for electron-beam evaporation, ion etching, Auger electron spectroscopy (AES), and low energy electron diffraction (LEED). The layers were degassed in UHV at 1073 K, where the N$_2$ vapor pressure over TiN is less than 10^{-10} Torr [11], for approximately 1200 s. Epitaxial TiN(111) buffer layers, 50–100 Å thick, were deposited at 1023 K in the STM chamber by reactive evaporation from Ti rods in 1×10^{-7} Torr N$_2$ and annealed in N$_2$ for 4 h at $T_a \simeq 1100$ K. This procedure resulted in sharp 1×1 LEED patterns corresponding to an in-plane atomic spacing of 2.99 Å and an STM-measured step height of 2.4 Å, both equal to

expected values for bulk TiN [12]. AES analyses show that the samples contain $\simeq 2$ mole % oxygen, probably in the form of TiO which is isostructural [12] and mutually soluble with TiN.

Partial TiN(111) bilayers (BL) [13] with coverages of 0.5 to 0.8 BL were deposited on TiN(111)/Al$_2$O$_3$($11\bar{2}0$) substrates by reactive evaporation at room temperature. The samples were then annealed *in situ* at $T_a = 1150-1250$ K in 1×10^{-7} Torr N$_2$ for times $t_a = 1-2$ h. This results in $\simeq 500$-Å-wide atomically smooth terraces (separated by bilayer-height steps) with truncated-triangular-shaped 2D TiN(111) vacancy islands whose average radii range from 50 to 260 Å. At each T_a, several series of STM images of individual vacancy islands were acquired as a function of t_a at a constant rate (18 to 44 s per frame). The sample and tip were allowed to stabilize thermally at T_a for 2 to 3 h prior to obtaining the STM images (pixel resolution varied from 1.25×1.25 to 2.5×2.5 Å^2). Typical tunneling conditions were 0.4–0.6 nA at -3.5 V. Scan sizes, scan rates, and tunneling parameters were varied to check for tip induced effects. No such effects were observed in results presented here.

For each of the measurement sequences, island boundaries and areas were determined from the STM images using Image SXM, an image processing software [14]. Ostwald ripening leading to island coarsening and decay [15] was observed during the annealing experiments. Since analysis of island shape fluctuations requires islands of nearly constant area [7,8], only data from consecutive scans with a maximum total change in area of $\leq 10\%$ were used and the boundary coordinates $r(\theta, t_a)$ of measured islands were normalized to the smallest island area in the measurement sequence [16]. The equilibrium island shape $R(\theta)$ is obtained by averaging $r(\theta, t_a)$ at all t_a values; i.e., $R(\theta) \equiv \langle r(\theta, t_a)\rangle$. For convenience, the symbols R and r in the following discussion refer to $R(\theta)$ and $r(\theta, t_a)$, respectively.

Figures 1a and 1b are consecutive STM images of a TiN(111) 2D vacancy island acquired at 1200 K while scanning at 32 s per frame. The observed changes in island shape are due to thermal fluctuations. The equilibrium
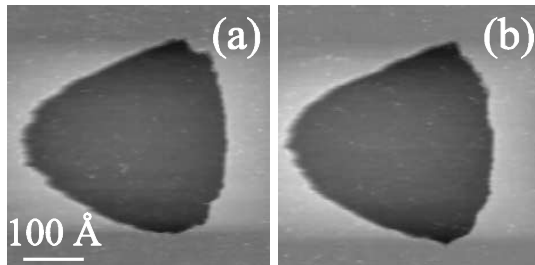
island shape R, obtained from the average of all images (typically 15–40) in a given measurement sequence, was fit with Lorentzian functions [17] of the general form,

$$R = R_0 + a/[1 + b(\theta - \theta_c)^2], \tag{1}$$

where R_0, a, b, and θ_c are fitting parameters. Figure 2a shows a plot of R vs θ obtained at 1200 K (open circles) and the analytical fit obtained using Eq. (1) (solid line). Analytical fits to all experimental data provide equally good agreement.

The inverse Legendre transform of R yields relative values of $\beta(\varphi)$ through the relation $\beta(\varphi) = \lambda R \cos(\varphi - \theta)$ [3]. Note that φ is the local normal to the equilibrium shape at R and is given by $\varphi = \theta - \arctan(\dot{R}/R)$ [3,8,18], where $\dot{R}$ denotes the first spatial derivative of R with respect to θ. Substituting for φ, we obtain an analytical expression for $\beta(\varphi)$ in terms of R as

$$\beta(\varphi) = \lambda \frac{R^2}{\sqrt{R^2 + \dot{R}^2}}. \tag{2}$$

Fits to the equilibrium shape R in Eq. (1) yield $\beta(\varphi)$ directly from Eq. (2). A polar plot of $\beta(\varphi)$ (dotted line) calculated with $\lambda = 1$ is shown in Fig. 2b. The two $\langle 110\rangle$ steps are labeled as S_1 and S_2. The ratio of step energies, β_1/β_2 (i.e., the maximum variation of β with φ) obtained using Eq. (2) is 0.72. From measurements of a total of 17 vacancy islands, the temperature- and size-dependent changes in this ratio over the range $T_a = 1165-1248$ K were found to be $<5\%$. In the following discussion we present results obtained only at $T_a = 1200$ K.

In order to determine λ and, hence, absolute $\beta(\varphi)$ values, we first generalize the isotropic theory of shape fluctuations proposed in Ref. [8] to treat anisotropic island shapes. Then, we apply the new theory to analyze the STM fluctuation measurements and obtain λ for TiN(111).

The total free energy F of an island is related to the island shape r through the relationship

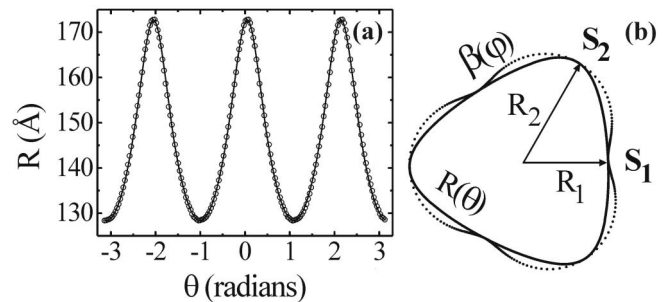$$F = \int_0^{2\pi} \{\beta[\varphi(\theta, t_a)](r^2 + \dot{r}^2)^{1/2}\} d\theta. \tag{3}$$

FIG. 1. (a) and (b): Consecutive STM images (430×430 Å^2) of a 2D vacancy island on an atomically smooth TiN(111) terrace. The images were acquired during annealing at $T_a = 1200$ K.

FIG. 2. (a) R vs θ plot of the measured equilibrium island shape (open circles) fit with Eq. (1) (solid line). (b) Polar plot of $R(\theta)$ (solid line) and $\beta(\varphi)$ (dotted line) derived from $R(\theta)$ using Eq. (2) with $\lambda = 1$. S_1 and S_2 are the two $\langle 110\rangle$ close-packed steps bounding the island.

Note that the angle $\varphi(\theta, t_a)$ in Eq. (3) is the local normal to the fluctuating shape at $r(\theta, t_a)$ in contrast to Eq. (2), where φ corresponds to the local normal to the equilibrium shape at $R(\theta)$. Thus, $\beta(\varphi)$ in Eq. (3) is also a function of r and hence t_a. Since the equilibrium shape corresponds to the minimum free energy F_0, temporal deviations $g(\theta, t_a)$ from the equilibrium shape result in a change in free energy $\Delta F \equiv F - F_0$, where we have defined $g \equiv g(\theta, t_a)$ (as in Refs. [7,8]) to be the normalized deviation of the temporal shape r from the equilibrium shape R. Thus, $g \equiv [r - R]/R$.

In order to derive an expression for λ in terms of the measurable quantity g, we construct a function $f \equiv f(\theta, r, \dot{r})$ defined as

$$f(\theta, r, \dot{r}) = \beta[\varphi(t_a)](r^2 + \dot{r}^2)^{1/2} - \lambda(r^2/2). \quad (4)$$

The second term in Eq. (4) accounts for the constant area constraint with a Lagrange multiplier λ. Expanding f to second order by Taylor's theorem for functions of two variables (r and $\dot{r}$) and substituting for $\beta(\varphi)$ from Eq. (2), we derive an expression for ΔF in terms of λ and g,

$$\Delta F = \frac{\lambda}{2}\left(\int_0^{2\pi}[\chi(\theta, t_a)]^2\, d\theta - \int_0^{2\pi}[\rho(\theta, t_a)]^2\, d\theta\right), \quad (5)$$

where we define $\chi(\theta, t_a)$ and $\rho(\theta, t_a)$ as

$$\chi(\theta, t_a) \equiv R^2 \dot{g}/(R^2 + 2\dot{R}^2 - R\ddot{R})^{1/2} \quad \text{and}$$

$$\rho(\theta, t_a) \equiv gR. \quad (6)$$

In Eq. (6), $\ddot{R}$ denotes the second derivative of R with respect to θ. Rewriting the functions as Fourier series $\chi(\theta, t_a) = \sum_n \chi_n(t_a)e^{in\theta}$ and $\rho(\theta, t_a) = \sum_n \rho_n(t_a)e^{in\theta}$ allows Eq. (5) to be expressed in terms of the Fourier components χ_n and ρ_n as $\Delta F = \pi\lambda \sum_n G_n$ in which $G_n = |\chi_n(t_a)|^2 - |\rho_n(t_a)|^2$. Since temporal changes in the total free energy are only due to g, ΔF can be expressed as a homogeneous second-order function in $\{g_n\}$, where $g_n \equiv (1/2\pi)\int_0^{2\pi} g e^{-in\theta}\, d\theta$. Then, by Euler's theorem, we obtain $\sum_n g_n(\partial\Delta F/\partial g_n) = 2\Delta F$. Comparing the above relation to the generalized equipartition theorem [19], we find that the time-averaged free energy $\langle\Delta F\rangle$ is equal to $N_{\max}k_B T/2$, where $N_{\max}$ corresponds to the maximum number of allowable fluctuation modes [20]. Thus, we obtain λ as

$$\lambda = \frac{N_{\max}k_B T}{2\pi \sum_n \langle G_n\rangle}. \quad (7)$$

We have measured the temporal fluctuations of eight vacancy islands of average radii ranging from 50 to 260 Å at 1200 K. For each island, the equilibrium shape R and g were determined from the STM data. $\chi(\theta, t_a)$ and $\rho(\theta, t_a)$ values were calculated numerically based upon Eq. (6) using the analytical fits to $R(\theta)$ of Eq. (1). The calculated Fourier components G_n were then used in Eq. (7) in order to obtain λ values for all islands. Substituting

the size-dependent values for λ into Eq. (2), we determine absolute values for $\beta(\varphi)$: $\beta_1 = 0.21 \pm 0.04$ and $\beta_2 = 0.29 \pm 0.06$ eV/Å.

The step-edge stiffness $\tilde{\beta}(\varphi)$ is related to the curvature $\kappa(\theta)$ of the equilibrium shape through the expression $\tilde{\beta}(\varphi) = \lambda/\kappa(\theta)$, where $\kappa(\theta) = (R^2 + 2\dot{R}^2 - R\ddot{R})/(R^2 + \dot{R}^2)^{3/2}$. $\kappa(\theta)$ was calculated for all islands to obtain step-edge stiffnesses of $\tilde{\beta}_1 = 1.5 \pm 0.6$ and $\tilde{\beta}_2 = 0.07 \pm 0.01$ eV/Å.

In the unrestricted terrace-step-kink model, $\tilde{\beta}$ is related to the kink formation energy ε on a close-packed step as [21]

$$\tilde{\beta} = (2a_\| k_B T/a_\perp^2)\sinh^2(\varepsilon/2k_B T), \quad (8)$$

where $a_\| = 2.99$ Å and $a_\perp = (\sqrt{3}/2)a_\| = 2.59$ Å are the unit lattice spacing parallel and orthogonal to the step edge, respectively. ε was determined for steps S_1 and S_2 on all islands. Average kink formation energies are $\varepsilon_1 = 0.43 \pm 0.04$ and $\varepsilon_2 = 0.16 \pm 0.01$ eV. Essentially identical results, $\varepsilon_1 = 0.43 \pm 0.04$ and $\varepsilon_2 = 0.13 \pm 0.01$ eV, are obtained using a formulation recently derived by Emundts *et al.* [22] based upon Akutsu and Akutsu's hexagonal lattice model [23].

Finally, we note that the entropic contribution to the step energies on metal surfaces is of order $(k_B T/a_\|)\ln[\coth(\varepsilon/2k_B T)]$ [21] and generally ignored [6,7]. Using $\varepsilon = 0.43$ eV in the above expression, we estimate the entropic contribution to be $\simeq -1.0 \times 10^{-3}$ eV/Å at 1200 K, which is much smaller than the statistical uncertainties (0.04 and 0.06 eV/Å for S_1 and S_2, respectively). Regarding the effect of pixel resolution on the determination of step energies, it has been reported that a systematic experimental uncertainty introduced into the fluctuation measurements due to the limited spatial resolution is of order $\frac{1}{2}$ of a pixel width [7]. Applying this result, we estimate a maximum uncertainty in step energies due to this effect of $\simeq 5\%$. This is less than the statistical uncertainty noted above.

In conclusion, *in situ* STM was used to measure shape fluctuations around the equilibrium shape of 2D TiN(111) vacancy islands at temperatures between 1165 and 1248 K. TiN(111) islands are highly anisotropic with $\beta_1/\beta_2 = 0.72 \pm 0.02$ at $T_a \simeq 1200$ K ($\simeq 0.38T_m$ [24]). We have derived and implemented a new approach for the analysis of shape fluctuations, applicable to both isotropic and highly anisotropic islands, to determine absolute step energies $\beta_1 = 0.21 \pm 0.04$ and $\beta_2 = 0.29 \pm 0.06$ eV/Å, step stiffnesses $\tilde{\beta}_1 = 1.5 \pm 0.6$ and $\tilde{\beta}_2 = 0.07 \pm 0.01$ eV/Å, and kink formation energies $\varepsilon_1 = 0.43 \pm 0.04$ and $\varepsilon_2 = 0.16 \pm 0.01$ eV.

[1] F. H. Baumann, D. L. Chopp, T. Díaz de la Rubia, G. H. Gilmer, J. E. Greene, H. Huang, S. Kodambaka, P. O'Sullivan, and I. Petrov, MRS Bull. **26**, 182 (2001).

[2] W. W. Mullins, Interface Sci. **9**, 9 (2001); H. van Beijeren and I. Nolden, in *Topics in Current Physics* (Springer-Verlag, Berlin, New York, 1987), Vol. 43, p. 259; M. Wortis, in *Chemistry and Physics of Solid Surfaces VII,* edited by R. Vanselow and R. F. Howe (Springer, New York, 1988), p. 367.

[3] P. Nozières, in *Solids Far From Equilibrium,* edited by C. Godrèche (Cambridge University Press, Cambridge, United Kingdom, 1992), p. 1.

[4] N. C. Bartelt, R. M. Tromp, and E. D. Williams, Phys. Rev. Lett. **73**, 1656 (1994).

[5] K. Arenhold, S. Surnev, H. P. Bonzel, and P. Wynblatt, Surf. Sci. **424**, 271 (1999); H. P. Bonzel and A. Emundts, Phys. Rev. Lett. **84**, 5804 (2000).

[6] G. S. Icking-Konert, M. Giesen, and H. Ibach, Phys. Rev. Lett. **83**, 3880 (1999); M. Giesen, C. Steimer, and H. Ibach, Surf. Sci. **471**, 80 (2001).

[7] (a) D. C. Schlößer, L. K. Verheij, G. Rosenfeld, and G. Comsa, Phys. Rev. Lett. **82**, 3843 (1999); (b) C. Steimer, M. Giesen, L. Verheij, and H. Ibach, Phys. Rev. B **64**, 085416 (2001).

[8] S. V. Khare and T. L. Einstein, Phys. Rev. B **54**, 11 752 (1996).

[9] J. E. Greene, J.-E. Sundgren, L. Hultman, I. Petrov, and D. B. Bergstrom, Appl. Phys. Lett. **67**, 2928 (1995).

[10] I. Petrov, F. Adibi, J. E. Greene, W. D. Sproul, and W.-D. Münz, J. Vac. Sci. Technol. A **10**, 3283 (1992).

[11] K. Zeng and R. Schmid-Fetzer, Z. Metallkd. **87**, 540 (1996).

[12] Inorganic Index to Powder Diffraction File (Joint Committee on Powder Diffraction Standards, PA, 1997): Card numbers 38-1420 and 08-0117 for TiN and TiO, respectively.

[13] The [111] direction in B1-NaCl structure TiN is polar, consisting of alternating layers of Ti and N atoms.

[14] Image SXM, developed by Professor Steve Barrett, Liverpool, U.K. (http://reg.ssci.liv.ac.uk).

[15] S. Kodambaka, V. Petrova, A. Vailionis, P. Desjardins, D. G. Cahill, I. Petrov, and J. E. Greene, Thin Solid Films **392**, 164 (2001).

[16] With this procedure, the maximum uncertainty in step energies is estimated to be $\simeq 13\%$.

[17] Measured $R(\theta)$ data at θ values in the range 0 to $2\pi/3$ were fit with two Lorentzian functions. By symmetry, the same set of functions, with θ_c shifted by $2\pi/3$ and $4\pi/3$, was used to fit the data at higher θ values. Note that the form of Eq. (1) provides an analytical means to calculate $\dot{R}$ and $\ddot{R}$ and has no physical significance.

[18] S. Kodambaka, S. V. Khare, D. D. Johnson, I. Petrov, and J. E. Greene (to be published).

[19] K. Huang, *Statistical Mechanics* (Wiley, New York, 1963), p. 149.

[20] With the smallest mode corresponding to two surface-atom spacings [Ref. [7(a)]], $N_{\max}$ is defined as one-half of the total number of atoms along the island periphery.

[21] N. C. Bartelt, T. L. Einstein, and E. D. Williams, Surf. Sci. **276**, 308 (1992); E. D. Williams, R. J. Phaneuf, J. Wei, N. C. Bartelt, and T. L. Einstein, Surf. Sci. **294**, 219 (1993).

[22] A. Emundts, M. Nowicki, and H. P. Bonzel, Surf. Sci. **496**, L35 (2002).

[23] N. Akutsu and Y. Akutsu, J. Phys. Condens. Matter **11**, 6635 (1999).

[24] *CRC Handbook of Chemistry and Physics, 2001–2002* (CRC Press, Boca Raton, FL, 2001), 82nd ed., pp. 4–91.